

Muon spin rotation in the magnetic and superconducting ground states of (U,Th)Be₁₃ and (U,Th)Pt₃

R. H. Heffner, D. W. Cooke, A. L. Giorgi, R. L. Hutson, M. E. Schillaci,
H. D. Rempp, J. L. Smith, and J. O. Willis
Los Alamos National Laboratory, Los Alamos, New Mexico 87545

D. E. MacLaughlin
University of California, Riverside, California 92521

C. Boekema
San Jose State University, San Jose, California 95192

R. L. Lichti
Texas Tech University, Lubbock, Texas 79409

J. Oostens
University of Cincinnati, Cincinnati, Ohio 45221

A. B. Denison
University of Wyoming, Laramie, Wyoming 82071

(Received 7 November 1988)

Microscopic aspects of magnetism and superconductivity have been studied in the heavy-fermion superconducting alloy systems (U,Th)Be₁₃ and (U,Th)Pt₃ using the technique of positive-muon (μ^+) spin rotation and relaxation (μ SR). In U_{1-x}Th_xBe₁₃, $x=0.033$, a striking increase of zero-field Kubo-Toyabe relaxation rate σ_{KT} is observed below the temperature $T_{c2} \approx 0.4$ K at which a second phase transition occurs in the superconducting state. This jump is firm evidence for the onset of weak static magnetism below T_{c2} . The observed increase of ~ 1.5 Oe in the μ^+ local field corresponds to an effective moment of 10^{-3} – 10^{-2} μ_B /U atom. The μ^+ Knight shift K_μ in the normal states of U_{1-x}Th_xBe₁₃, $x=0$ and 0.033, is proportional to the bulk susceptibility and yields a transferred f -spin- μ^+ hyperfine field of -1.99 ± 0.12 kOe/ μ_B . In the superconducting states of U_{1-x}Th_xBe₁₃, $x=0$, 0.01, and 0.033, a large reduction of the magnitude of K_μ is observed for $x=0$ but not for $x=0.033$, and an intermediate reduction is found for $x=0.01$. This behavior suggests (1) spin-singlet pairing in undoped UBe₁₃, and (2) conventional reduction of the spin susceptibility suppression in (U,Th)Be₁₃ by spin-orbit scattering from Th impurities. In undoped UPt₃ small increases of σ_{KT} and the transverse-field Gaussian relaxation rate σ_G below ~ 6 K are again evidence for the onset of weak static magnetism similar to that found in (U,Th)Be₁₃. Recent spin-polarized neutron scattering studies of normal-state UPt₃ have observed a commensurate antiferromagnetic (AF) structure with a sublattice magnetization of $\sim 10^{-2}$ μ_B /U atom, in rough agreement with the μ SR results. For U_{1-x}Th_xPt₃, $x=0.05$, zero-field μ^+ precession frequencies below 6.5 K indicate an AF structure with a considerably larger moment (~ 0.6 μ_B /U atom). The average μ^+ Knight shift in the normal state of undoped UPt₃ is much smaller than in UBe₁₃, which suggests multiple μ^+ stopping sites with hyperfine couplings of opposite signs.

I. INTRODUCTION

Despite a great deal of experimental¹ and theoretical² effort over the past several years, the precise nature of the so-called heavy-fermion (HF) state of condensed matter is still not completely understood. Heavy-fermion materials contain certain $4f$ or $5f$ elements (e.g., Ce, U) and exhibit many intriguing properties. At high temperatures the magnetic susceptibility is paramagnetic and shows Curie-Weiss-like behavior, which indicates the existence of weakly interacting localized f -electron moments. Below a characteristic temperature $T_0 \sim 10$ – 100 K these local moments disappear, leaving in their place strongly interacting itinerant electrons with large effective masses

($\sim 100 \times$ free-electron mass). This large effective mass is manifested through a large linear specific-heat coefficient γ . The susceptibility χ also becomes large and temperature independent (Pauli-like) at low temperatures, such that the Wilson ratio γ/χ is approximately the free-electron value. Coherent electron scattering is observed, e.g., as a decreasing resistivity, as the temperature is lowered below a "coherence" temperature $T_{coh} \ll T_0$. The HF state can be paramagnetic (CeAl₃, CeCu₆), magnetically ordered (UCd₁₁, NpBe₁₃, URu₂Si₂), or superconducting (UPt₃, UBe₁₃, CeCu₂Si₂) and, in some compounds (URu₂Si₂), exhibits both an antiferromagnetic (AF) and a superconducting phase transition.

Of particular interest are the unusual superconducting

properties of the heavy-fermion compounds UBe_{13} and UPt_3 . The superconducting energy gaps of these materials are highly anisotropic,^{1,2} vanishing either at points (UBe_{13} , applied field $H_0=0$) or on lines (UPt_3 ; UBe_{13} , $H_0 \gtrsim 1.5T$ Ref. 3) on the Fermi surface. These properties, together with very large values of the upper critical field H_{c2} and its slope $-(dH_{c2}/dT)_{T_c}$ at T_c ,¹ have led many investigators to conclude that the HF superconducting state is not the same as in the phonon-mediated BCS superconductors previously studied. The pairing mechanism itself is therefore likely to be unconventional, and may involve the exchange of purely electronic excitations rather than phonons.

In addition, the nature of the HF state is very sensitive to impurity doping. For example, addition of a few atomic percent (at. %) thorium⁴ or palladium⁵ to UPt_3 introduces or enhances a Fermi surface instability below 5–6 K, which results in a commensurate AFM structure⁶ with a moment of about 0.5 Bohr magneton (μ_B). Similar concentrations of Th in UBe_{13} produce a nonmonotonic depression of the superconducting transition temperature T_{c1} with increasing Th concentration.⁷ For Th concentrations between ~ 2 and ~ 4 at. % in $(\text{U,Th})\text{Be}_{13}$ the specific heat⁸ indicates a second phase transition at a temperature T_{c2} below the superconducting transition at T_{c1} . Ultrasonic experiments⁹ suggest that this second transition is to a spin-density wave state, but no evidence for magnetic order has been obtained from either neutron scattering¹⁰ or NMR (Ref. 11) experiments.

In this paper we report studies of the magnetic and superconducting properties of $(\text{U,Th})\text{Be}_{13}$ and $(\text{U,Th})\text{Pt}_3$ alloys using the technique of muon-spin rotation and relaxation (μSR).¹² The muon possesses a relatively large magnetic dipole moment (3.2 times the nuclear magneton) and zero electric quadrupole moment; these two properties render μSR experiments particularly sensitive to small changes in local magnetic fields, so that muon linewidth changes and frequency shifts can be accurately determined. In the absence of spin-lattice relaxation or other dynamic contributions (as is the case in virtually all the present experiments), the muon relaxation rate reflects the distribution of microscopic local magnetic fields at the muon site or sites. The muon Knight shift, defined as the shift of precession frequency in a metallic environment, is a measure of the spin susceptibility in both the normal and the superconducting states. The temperature dependence of the latter gives information on the pairing mechanism. μSR investigations of a number of HF materials have been reported.^{13–18}

The paper is organized as follows: Our experimental procedures are described in Sec. II. Sections III and IV give the data and analysis for UBe_{13} - and UPt_3 -based systems, respectively. A summary and concluding remarks are presented in Sec. V. Part of this work has been published in preliminary form elsewhere.^{19–22}

II. EXPERIMENTAL PROCEDURES

Our μSR experiments were carried out at the Clinton P. Anderson Meson Physics Facility (LAMPF), Los

Alamos National Laboratory. A beam of positive muons (μ^+) from the backward decay of in-flight pions, with a spin polarization of $\sim 85\%$ and a momentum of 80 MeV/c, was implanted in samples of interest, and the subsequent precession and relaxation of the μ^+ polarization was observed.

A standard time-differential μSR spectrometer,¹² shown schematically in Fig. 1, was used. A pair of Helmholtz coils produced applied magnetic fields between 0 and 5 kOe at the sample position. For zero-field experiments any stray fields were nulled to $\lesssim 0.01$ Oe using three pairs of mutually perpendicular bucking coils. The Helmholtz pair could be rotated to orient the applied field \mathbf{H}_0 either parallel or perpendicular to the muon-spin polarization \mathbf{S}_μ , which was directed along the beam axis. The parallel configuration, shown in Fig. 1, was also used for experiments in zero field. In this configuration a second small Helmholtz pair produced a field oriented perpendicular to the muon-spin polarization. Transverse μSR in this field was used to determine asymmetry and normalization parameters as discussed below. For Knight-shift measurements^{12,23} the field stability was monitored by a NMR probe, and an absolute field calibration was obtained by measuring the muon precession frequency of a standard copper sample with a known²³ Knight shift of 60 ppm.

The data acquisition electronics were configured as shown schematically in Fig. 2 which, with Fig. 1, defines all counter nomenclature used below. The signal MU for a muon stop in the sample S was defined as a coincidence (logical AND) of the BE and M counters, together with no coincident signal from the SBOX array. SBOX was

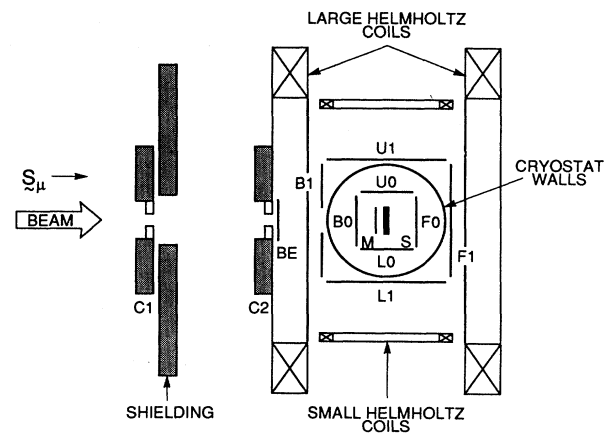


FIG. 1. Diagram of the μSR spectrometer in the parallel configuration (applied field \mathbf{H}_0 parallel to muon-spin direction \mathbf{S}_μ). Collimators $C1$ and $C2$ help to focus the muon beam on the sample S . Incident muons are counted by counters BE and M . Positron counters are labeled $F0$ and $F1$ (front), $B0$ and $B1$ (back), $L0$ and $L1$ (lower), and $U0$ and $U1$ (upper). Small Helmholtz coils were used to produce a transverse field (~ 100 Oe) to determine asymmetry and normalization parameters in the parallel configuration shown. For zero-field measurements the field at S could be reduced to $\lesssim 10$ mOe using three pairs of orthogonal coils (not shown).

defined as the logical OR signal from the $U0$, $F0$, or $L0$ counters. The macroscopic LAMPF duty factor of 6–9% put severe constraints on the average muon stopping rates, so that the rate of undesired two-muon events within the time window of 8–12 μs (referred to as “pile-up”) would be minimized. Pileup rejection [Pu R in Fig. 2(b)] was implemented for the MU signal. As a practical matter the MU rate was limited to 1.2 kHz average (20 kHz instantaneous) for a 6% accelerator duty factor, in order to keep the random background rate to less than a few percent of the signal. The M , $B0$, $U0$, $F0$, and $L0$ counters were placed in the cryostat vacuum space, to reduce the number of MU signals from muons stopping in the cryostat materials.

A positron signal was defined as a coincidence between all the counters in one and only one position telescope [$N=1$ in Fig. 2(b)]. Two counters per telescope, as shown in Fig. 1, were used with the dilution refrigerator, and three counters per telescope were used with the gas-flow cryostat. A BE anticoincidence signal was used to veto positron events arising from decay of muons stopped in the $C2$ beam collimator.

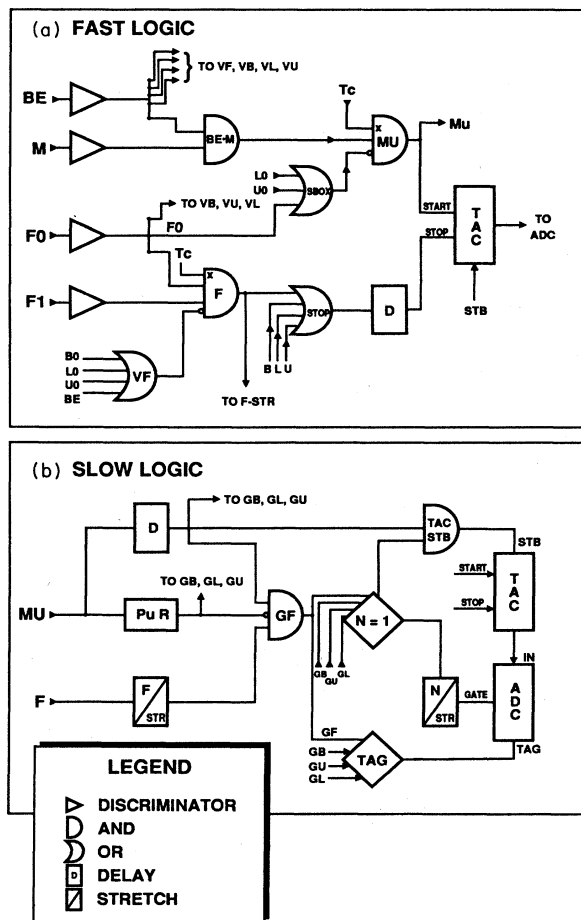


FIG. 2. Schematic diagram of the μSR data acquisition electronics. (a) Fast logic. (b) Slow logic. For clarity only the front counter logic is shown explicitly.

The time differences between muon stops and positron signals were collected in time-differential histograms, one histogram per positron telescope. Data were digitized by an Ortec time-to-amplitude converter (TAC), which fed a LeCroy analog-to-digital converter (ADC). Tag bits, which identified which of the four positron telescopes had fired, were also included in the 16-bit ADC word. The linearity and drift of the electronics were monitored by an Ortec time calibrator (TC), and were found to be stable to one part in 10^4 or better.

Time calibration runs (channel number versus real time) were taken several times a day for relaxation rate studies and every other data run for Knight-shift studies. A typical run required between 1 and 2 h to accumulate $\sim 5 \times 10^5$ events per histogram. Zero-time channels, corresponding to immediate muon decay, were measured using muons which passed through the sample area with the SBOX veto disabled. The counter system outside the cryostat could be rotated 90° to determine zero-time channels for counter telescopes perpendicular to the muon beam.

The time-differential histogram rates $N(t)$ for each telescope were fit to the general form¹²

$$N(t) = B + N_0 e^{-t/\tau_\mu} [1 + aG(t)\cos(\omega_\mu t + \phi)] \quad (1)$$

Here B is a time-independent background term, N_0 is the initial counting rate, τ_μ is the muon decay time constant, a is the product of the μ^+ beam polarization and the geometrical asymmetry, $G(t)$ is the normalized relaxation function, ω_μ is the muon Larmor frequency, and ϕ is a phase angle. The value $\tau_\mu = 2.20 \mu\text{s}$ was fixed for all telescopes. In the parallel configuration $\omega_\mu = 0$ and $\phi = 0$ and π for the front and back histograms respectively, so that $\cos(\omega_\mu t + \phi) = \pm 1$.

Parallel-configuration data could be fit using either of two methods. In the first method histograms from the front (+) and (–) telescopes (cf. Fig. 1) were simultaneously and separately fit to Eq. (1) using a common relaxation function $G(t)$. The asymmetries a_+ and a_- were determined from separate “normalization” runs taken in a low (100 Oe) transverse field. Typically $a_+ \approx a_- \approx 0.2$ and $B_\pm/N_{0\pm} \approx 0.02$.

In the second fitting method, an asymmetry function $R(t)$ was formed from the two histograms as follows:

$$R(t) = \frac{N_+(t) - \alpha N_-(t)}{a_- N_+(t) + a_+ \alpha N_-(t)} \quad (2)$$

Here $N_+(t)$ and $N_-(t)$ are the front and back histogram rates after subtraction of the backgrounds B_\pm . The parameter $\alpha = N_{0+}/N_{0-}$, like the asymmetries, was determined experimentally from transverse-field normalization runs; typically $\alpha \approx 1$.

Ideally $R(t) = G(t)$. In practice small drifts between normalization runs forced us to fit the experimental asymmetry function $R^{\text{expt}}(t)$ to the form

$$R^{\text{expt}}(t) = R(t) + \delta B, \quad (3)$$

where δB is a small change in background. It was found, moreover, that the normalization parameter α , determined from separate transverse-field runs as described

above, varied from run to run unless the MU rate was kept to ≈ 1.2 kHz average. The value of α could be self-consistently determined for a given run by fitting the raw histograms separately to Eq. (1), but then the statistical uncertainty in relaxation-function parameters was unacceptably large (larger than for fits of $R^{(\text{expt})}(t)$ [Eq. (3)] to asymmetry functions).

Sample temperatures were controlled using a Helitran gas-flow cryostat for temperatures between ~ 3 and 300 K, and by a ^3He - ^4He dilution refrigerator developed at LAMPF (Ref. 24) for temperatures between 0.2 and 3 K. In both cryostats the sample was thermally anchored to a silver rod attached to the refrigerating element (Helitran cold finger or dilution refrigerator mixing chamber). Sample temperatures were monitored using carbon-glass thermometers thermally anchored to the sample itself.

The samples were prepared by arc melting stoichiometric quantities of the constituents in elemental form. For the doped samples single pieces of the dopant elements were used to ensure that no material was lost. The arc furnace was evacuated while the UBe_{13} -based samples were still molten after the final melt; this effected a relatively slow anneal. The UPt_3 -based samples were wrapped in tantalum, sealed in quartz ampoules, and annealed for several days at 1250 °C. Superconducting transition temperatures were determined using ac susceptibility measurements. For $\text{U}_{1-x}\text{Th}_x\text{Be}_{13}$, $x=0, 0.01, \text{ and } 0.033$, $T_{c1}=0.86\pm 0.02$ K, 0.68 ± 0.02 K, and 0.60 ± 0.02 K, respectively. For our sample of UPt_3 $T_c=0.41\pm 0.01$ K.

III. EXPERIMENTAL RESULTS:

(U,Th) Be_{13}

We have carried out μ^+ relaxation and Knight-shift experiments in undoped UBe_{13} and in $\text{U}_{1-x}\text{Th}_x\text{Be}_{13}$, $x=0.01$ and 0.033 . These were motivated by the unusual superconducting behavior of this alloy system described in Sec. I, together with the known utility of implanted muons as interstitial probes of their magnetic environments. Weak static magnetism in $\text{U}_{1-x}\text{Th}_x\text{Be}_{13}$, initially suggested by an ultrasonic attenuation anomaly at T_{c2} ,⁹ can be sensed directly via the behavior of μ^+ local fields. Similarly, the Knight shift of spin probes (nuclei or muons) reflects the local spin susceptibility, and as a result can shed light on the nature of superconducting pairing which affects this susceptibility.

A. Relaxation rate studies

Figure 3 shows the temperature dependence of the Gaussian relaxation rate σ_G for undoped UBe_{13} in a 100-Oe transverse field. These data were obtained by fitting each histogram to Eq. (1) with $G(t)$ taken to be the Gaussian relaxation function $G_G(t)=\exp(-\frac{1}{2}\sigma_G^2 t^2)$. (Note that the relaxation rate is identical to the resonance linewidth; the two terms will be used synonymously.) Below $T\sim 150$ K a temperature-independent linewidth $\sigma_G=0.21\pm 0.01 \mu\text{s}^{-1}$ was obtained. Above about 150 K the linewidth decreases rapidly, due to the onset of thermally induced μ^+ diffusion and consequent motional narrowing.¹²

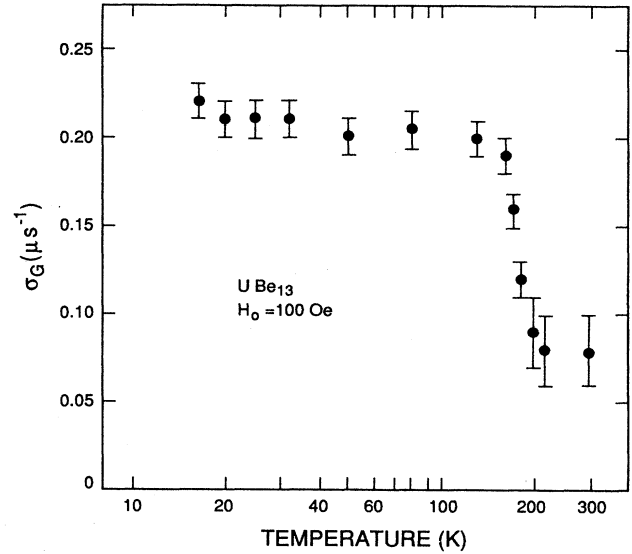


FIG. 3. Temperature dependence of the μ^+ transverse relaxation rate σ_G in UBe_{13} , applied field $H_0=100$ Oe.

Data taken in zero applied field were fit to the Kubo-Toyabe²⁵ relaxation function $G_{\text{KT}}(t)$, given by

$$G_{\text{KT}}(t) = \frac{1}{3} + \frac{2}{3}(1 - \sigma_{\text{KT}}^2 t^2) \exp(-\frac{1}{2}\sigma_{\text{KT}}^2 t^2). \quad (4)$$

A typical measured relaxation function ($\text{U}_{1-x}\text{Th}_x\text{Be}_{13}$, $x=0.033$, at $T=0.215$ K), together with the fitted function from Eq. (4) (solid line), are shown in Fig. 4. Despite the statistical uncertainty at long times, the initial Gaussian-like relaxation at earlier times is well determined.

The temperature dependence of σ_{KT} between ~ 0.15 and 2.5 K for UBe_{13} is shown in Fig. 5 (solid circles). Within statistical error σ_{KT} is independent of temperature below ~ 3 K, with an average value $\sigma_{\text{KT}}=0.200\pm 0.005 \mu\text{s}^{-1}$. From Figs. 3 and 5 it can be seen that σ_{KT} in zero field and σ_G in transverse fields are nearly equal at low temperatures.

The theory of μ^+ linewidth due to nuclear dipolar interactions¹² gives two limiting values of the linewidth in weak and strong applied field, respectively. In strong fields the nonsecular terms in the μ^+ -nuclear dipolar interaction are averaged out by nuclear spin precession, and one obtains the secular Van Vleck value σ_{VV} (averaged over orientations in a polycrystalline sample). In weak or zero field relaxation is due to the full dipolar Hamiltonian, and the relaxation rate is faster:²⁵ $\sigma_{\text{KT}}=\sqrt{5/2}\sigma_{\text{VV}}$. In UBe_{13} , however, the ^9Be nuclei are in sites of noncubic symmetry, and nuclear quadrupolar precession in the resulting nonzero electric field gradient (EFG) can average the nonsecular dipolar terms even in zero applied field. This effect was first studied in a cubic system (Cu metal),¹² where the EFG is induced by the electric charge of the muon itself. The approximate equality of σ_{KT} and σ_G suggests, therefore, that quadrupole effects dominate the zero-field linewidth. This is not surprising, because ^9Be NMR spectra yield a quadrupole

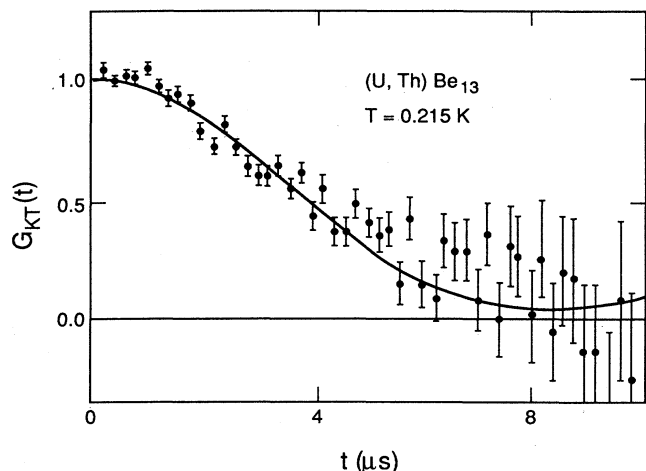


FIG. 4. Typical zero-field μ^+ relaxation function in $U_{1-x}Th_xBe_{13}$, $x=0.033$, $T=0.215$ K. The curve gives the best fit to the Kubo-Toyabe function $G_{KT}(t)$.

interaction of ~ 160 Oe in field units.²⁶ The 9Be nuclei are already in a large EFG even without any additional contribution from the muon, and for a small applied field of 100 Oe we expect $\sigma_G = \sigma_{KT}$ as observed.²⁵ The crystalline EFG at 9Be sites makes it difficult to identify the muon interstitial site or sites from the value of σ_G ; the conclusions of this paper are, however, independent of site identification.

As mentioned in the introduction to this section, studies of μ SR relaxation rates in $(U,Th)Be_{13}$ were undertaken in part to help resolve the nature of the second phase

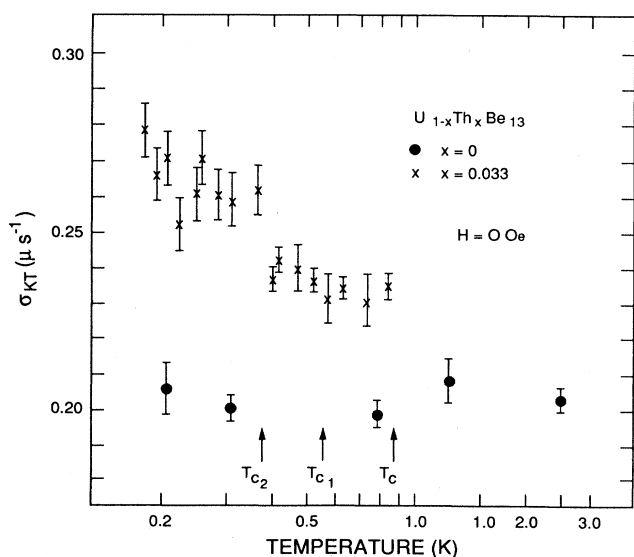


FIG. 5. Temperature dependence of the zero-field Kubo-Toyabe relaxation rate σ_{KT} in the normal and superconducting states of $U_{1-x}Th_xBe_{13}$, $x=0$ and 0.033 . The superconducting transition temperatures $T_c(x=0)$ and $T_{c1}(x=0.033)$ and the second transition temperature $T_{c2}(x=0.033)$ are shown by arrows.

transition,⁸ which occurs in the superconducting state of $U_{1-x}Th_xBe_{13}$ for $0.02 \lesssim x \lesssim 0.04$. The specific-heat jump associated with this transition reaches a maximum near $x=0.033$. Figure 6 gives the temperature dependence of the specific heat for our $x=0.033$ sample. The superconducting transition is clearly visible at $T_{c1} \simeq 0.55$ K, followed by a second transition at $T_{c2} \simeq 0.42$ K.

Batlogg *et al.*⁹ have taken the observed peak in ultrasonic attenuation at T_{c2} as evidence for an AF state which coexists with superconductivity below this temperature. Attempts to find evidence for such a state in neutron scattering¹⁰ or NMR (Ref. 11) experiments were not successful, however. The absence of any observed change in NMR spectra, which were dominated by quadrupolar broadening, placed an approximate upper limit of $10^{-2} \mu_B/U$ atom on the size of any magnetic moment below T_{c2} . We note that μ SR experiments can easily resolve line broadening due to nuclear magnetic moments, which are a factor of 10 smaller than this upper limit. In addition μ SR, unlike conventional NMR, can be carried out in zero applied field.

Comparison of the behavior of σ_{KT} for $U_{1-x}Th_xBe_{13}$, $x=0$ and 0.033 (Fig. 5), reveals important differences and similarities. First, neither compound exhibits a change in linewidth below the superconducting transition temperature T_{c1} . This is to be expected if the μ^+ local fields are due principally to dipolar coupling to surrounding nuclei, because this coupling is not affected by superconductivity. The increase in normal-state relaxation rate near $T=1$ K for $x=0.033$ is probably due to small changes in μ^+ sites produced by random locations of Th impurities, which alter the rms dipolar coupling to 9Be nuclei.

Second, and most striking, a measurable increase of σ_{KT} is observed below T_{c2} for the Th-doped sample. Within statistical error the line shape at the lowest temperatures below T_{c2} is still well described by Eq. (4), indicating that the additional relaxation is produced by quasi-static (rather than rapidly fluctuating) magnetic fields.

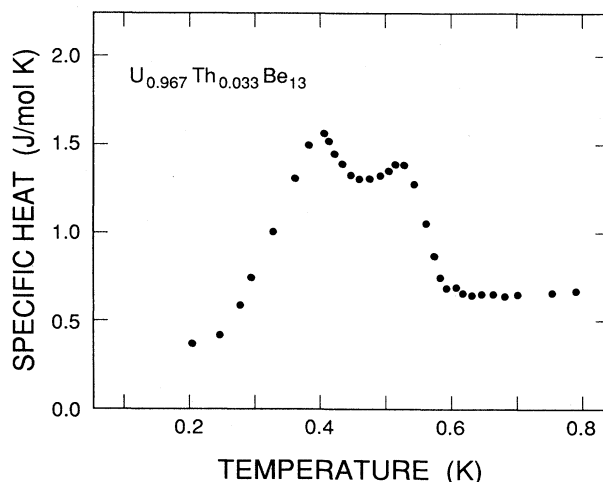


FIG. 6. Temperature dependence of the specific heat in our $U_{0.967}Th_{0.033}Be_{13}$ sample

(The term “quasistatic” refers to fluctuation times τ_c long compared to the inverse linewidth: $\sigma_{\text{KT}}\tau_c \gg 1$.) Such an increase in the linewidth (about 15% at the lowest temperature) can be due to only one of two causes: (1) a change in dipolar linewidth resulting from a structural phase transition, or (2) the onset of a small additional magnetic field. The first seems highly unlikely: the dipolar linewidth varies as r_i^{-3} , where r_i is the distance between the muon and the i th nucleus. Therefore a decrease in lattice parameters of $\sim 5\%$, which is 3 orders of magnitude larger than the observed change at T_{c2} ,²⁷ would be required to explain the measurement. We conclude that the increase of σ_{KT} below T_{c2} is firm evidence that the phase transition at this temperature is associated with weak electronic magnetism.

A rough estimate of ~ 1.5 Oe for the additional magnetic field at μ^+ sites below T_{c2} is obtained assuming that the additional field adds in quadrature with that due to nuclear dipoles. Assuming further that the coupling to localized magnetic moments is dipolar, and therefore of order 10^3 Oe/ μ_B at typical interatomic spacings and in the absence of symmetry restrictions (see below), this corresponds to an effective moment of about 10^{-3} μ_B /U atom. This small effective moment explains why the magnetic nature of the transition was not detected by either NMR or neutron scattering experiments. Although our estimate is smaller than that obtained from the ultrasonic absorption anomaly⁹ ($\sim 10^{-2}$ μ_B /U atom), the moment would have been observed by NMR or neutron scattering if it were more than an order of magnitude larger than 10^{-3} μ_B /U atom.

On the other hand, the increase of σ_{KT} due to AF ordering would be eliminated if muon sites were centered between commensurate AF sublattices, because dipolar or hyperfine fields from the two sublattices would then cancel. But in Th-doped samples the μ^+ sites might be slightly displaced due to the disordered electrostatic potential associated with the Th impurities, as noted above. Calculated dipolar lattice sums, based on this hypothesis and assuming displacements of a few percent, lead to a revised estimate of $\sim 10^{-2}$ μ_B /U atom, in qualitative agreement with the ultrasound results.

Unfortunately our results do not give a clear indication of the nature of the magnetic state, because a small increase in linewidth could be due to slightly increased inhomogeneous broadening on the one hand or coherent μ^+ precession in a weak but homogeneous field on the other. Thus a commensurate magnetic structure cannot be distinguished from an incommensurate one. (A large additional coherent precession is observed in $\text{U}_{0.95}\text{Th}_{0.05}\text{Pt}_3$, as discussed below in Sec. IV.) The question is important in part because of the possibility that a so-called “nonunitary” superconducting phase, in which Cooper pairs possess spin or orbital magnetism, sets in below T_{c2} . Such phases, which have been suggested by Volovik and Gor’kov²⁸ and studied recently by Sigrist and Rice,²⁹ would possess nonzero spin (for triplet pairing) and possibly nonzero orbital moment within a unit cell. This magnetism would then simulate magnetic ordering, and give rise to a local field at muon sites.

B. Knight-shift measurements

The relative frequency shift K of a spin probe (muon or nucleus) is in general a sum of terms, each of which corresponds to a particular interaction mechanism (contact, orbital, core polarization, etc.) between the spin probe and the corresponding contribution to the susceptibility χ . That is,³⁰

$$K = \sum_i K_i = \sum_i \alpha_i \chi_i, \quad \text{where } \chi = \sum_i \chi_i. \quad (5)$$

For a given susceptibility contribution the hyperfine field $H_{\text{hf}}^{(i)}$ is related to the slope $\alpha_i = dK_i/d\chi_i$ by $\alpha_i = H_{\text{hf}}^{(i)}/N\mu_B$, where N is the number of formula units per unit used in the susceptibility (i.e., N is Avogadro’s number for the molar susceptibility). In metals this frequency shift is often called the Knight shift, although strictly speaking that term should be reserved for contributions to K from itinerant electrons. Local moments can also make important and sometimes dominant contributions to K .

The spin-dependent contribution K_s from itinerant electrons is proportional to the itinerant-electron spin susceptibility χ_s in both the normal and superconducting states.³¹ Knight shifts in the superconducting state can therefore give information on the nature of superconducting pairing via its effect on χ_s . Early ²⁷Al Knight-shift measurements in superconducting aluminum³¹ confirmed the expected Yosida³² (BCS) temperature dependence of χ_s below T_c : $\chi_s(T)$ vanishes for $T \ll T_c$ in a superconductor with singlet pairing. If spin-orbit scattering is present conduction-electron spin eigenstates are mixed, so that Cooper pairing is no longer between states of well-defined spin. Then $\chi_s(T \ll T_c)$ is no longer zero, and approaches the normal-state value χ_n for the mean free path for spin-orbit scattering much less than the superconducting coherence length.³³ Spin-orbit scattering is expected to be important for superconductors containing high- Z elements, and has been observed in mercury and tin.³⁴ In a ³He-like model for spin-triplet superconductivity χ_s is also of order χ_n , although χ_s/χ_n can be reduced by Fermi-liquid corrections.³⁵ A complete theory of $\chi_s(T)$ in HF superconductors, where spin-orbit scattering of uranium-derived wave functions is expected to be large, has not yet been reported.

We have obtained μ^+ spectra in $\text{U}_{1-x}\text{Th}_x\text{Be}_{13}$, $x = 0, 0.01, \text{ and } 0.033$, over the temperature range $\sim 0.3\text{--}295$ K in a transverse applied field of 5 kOe. Fourier transforms of the histograms exhibited two frequency components (“lines”). Within errors the frequency of one of these lines was unshifted (compared to the Cu reference shift) and temperature independent. Auxiliary experiments showed that this unshifted line was due to muon stops in the cryostat walls. The loss of collimation was caused primarily by a spread in the incident beam momentum, which produced a spatial dispersion of the beam in the transverse applied field. A clean separation of the two lines was possible over most of the temperature range, but the presence of the background line limited the precision of the measurements, particularly that of the linewidths. Each frequency component of a histogram

was fit to an appropriately modified version of Eq. (1) with Gaussian relaxation functions. In the following we discuss only the frequency component with a temperature-dependent shift, for which the temperature dependence of the Gaussian linewidth has been published previously.¹⁹

When an applied field $H_0 > H_{c1}$ is applied to an ellipsoidal type-II superconducting sample with demagnetization factor n , the μ^+ spin in a μ SR experiment precesses at a frequency $\omega_\mu = \gamma_\mu B_\mu$, where $\gamma_\mu = 8.51 \times 10^4 \text{ s}^{-1} \text{ Oe}^{-1}$ is the muon gyromagnetic ratio and B_μ is the local magnetic induction at the μ^+ site. The experimentally measured shift $K_\mu^{(\text{expt})}$ is then given by $B_\mu/H_0 - 1$, and differs from K_μ by Lorentz, demagnetizing, and supercurrent screening corrections:

$$K_\mu^{(\text{expt})} = K_\mu + 4\pi(\frac{1}{3} - n)\chi_p + 4\pi\chi_d(1 - n), \quad (6)$$

where $\chi_p = \chi - \chi_d$ is the paramagnetic contribution to the total susceptibility, and χ_d is the diamagnetic susceptibility produced by persistent currents in the mixed-state vortex lattice. [In Eq. (6) the susceptibilities must be in dimensionless cgs units, i.e., emu cm^{-3} .] An accurate value of the intrinsic Knight shift K_μ can therefore be obtained only if the correction terms in Eq. (6) are small or can be determined independently. In the normal state only the paramagnetic correction [second term in Eq. (6)] is required.

The normal-state μ^+ Knight shifts K_μ in $\text{U}_{1-x}\text{Th}_x\text{Be}_{13}$, $x=0$ and 0.033 , are plotted versus the measured susceptibility χ , with temperature an implicit variable, in Fig. 7. These data have been corrected using Eq. (6) with $\chi_d=0$. (The corrections differ slightly from those in a preliminary version of this work.^{19,22}) One sees that K_μ is proportional to χ for $\chi \gtrsim 7 \times 10^{-3} \text{ emu mol}^{-1}$, which corresponds to temperatures $\lesssim 150 \text{ K}$. We attribute the lack of proportionality for $\chi \lesssim 7 \times 10^{-3} \text{ emu mol}^{-1}$ to rapid muon diffusion between inequivalent interstitial sites (Sec. III A). Muon diffusion above $\sim 150 \text{ K}$ is also clearly manifested in the temperature dependence of the μ^+ linewidth (Fig. 3).

For $\chi \gtrsim 7 \times 10^{-3} \text{ emu mol}^{-1}$ the data of Fig. 7 are well described by $K_\mu(T) = \alpha_0\chi_0 + \alpha_f\chi_f(T)$, where χ_0 sums all temperature-independent contributions to the susceptibility and $\chi_f(T)$, the f -electron susceptibility, is assumed to account for all of the temperature dependence of χ . The value of χ_0 found from the intercept of a plot of χ versus $1/T$ is $\approx 1 \times 10^{-3} \text{ emu mol}^{-1}$. We then obtain $K_\mu = (0.19 \pm 0.03)\%$ for $\chi_f=0$, as indicated on Fig. 7.

From the slope α_f of the straight line on Fig. 7 the f -electron hyperfine field $H_{\text{hf}}^{(f)}$ is found to be $(-1.99 \pm 0.12) \text{ kOe}/\mu_B$. This is similar to other values for f -electron- μ^+ transferred hyperfine fields in heavy-fermion materials.¹⁵ A value of about $20 \text{ kOe}/\mu_B$ is found for the hyperfine field corresponding to α_0 . This is consistent with contact-type μ^+ hyperfine fields found in typical metals,²³ although χ_0 is considerably larger than usual Pauli susceptibilities.

The temperature dependence of $K_\mu^{(\text{expt})}$ is given in Fig. 8 for $x=0$ and 0.033 . It is clear that below T_c the magnitude of the Knight shift is significantly reduced for

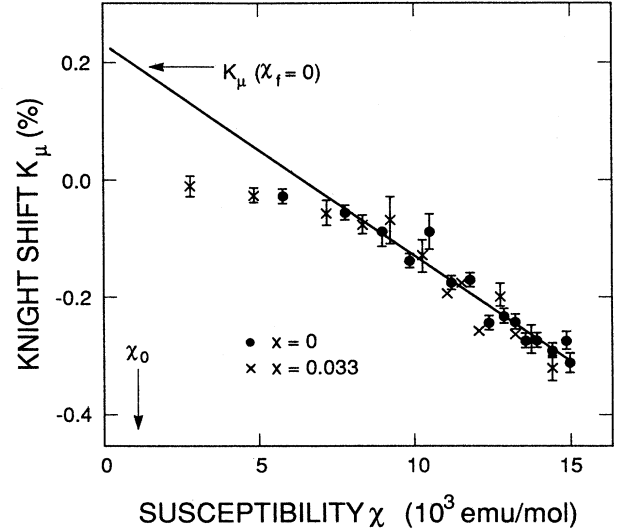


FIG. 7. Dependence of μ^+ Knight shift K_μ , corrected for Lorentz and demagnetizing fields, on bulk susceptibility χ in the normal states of $\text{U}_{1-x}\text{Th}_x\text{Be}_{13}$, $x=0$ and 0.033 . Temperature is an implicit variable. Refinement of the data has produced slight differences from the results reported in Ref. 13.

$x=0$ but not for $x=0.033$. We note that these data have not been corrected using Eq. (6), because χ has not been measured independently below T_c . One can nevertheless estimate these quantities, and draw qualitative conclusions regarding the nature of the Knight shifts.

We first estimate the diamagnetic corrections in pure UBe_{13} . In conventional Ginzburg-Landau theory³⁶ one has

$$-4\pi\chi_d = \frac{H_{c2}/H_0 - 1}{\beta(2\kappa^2 - 1) + n}, \quad (7)$$

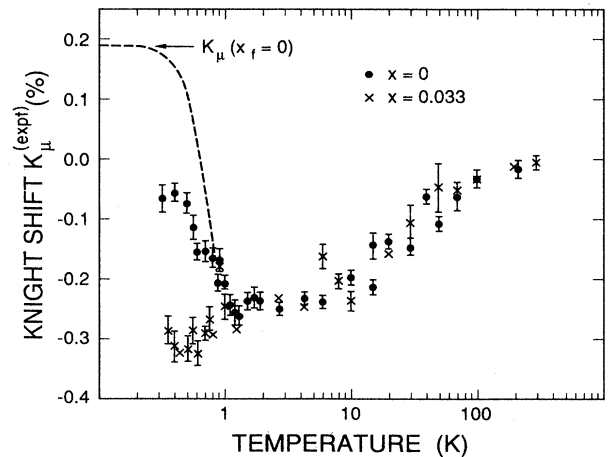


FIG. 8. Temperature dependence of measured μ^+ Knight shift $K_\mu^{(\text{expt})}$ in $\text{U}_{1-x}\text{Th}_x\text{Be}_{13}$, $x=0$ and 0.033 . The dashed curve gives the BCS (Yosida) temperature dependence for $K_\mu^{(\text{expt})}(\chi_f=0) = 0.19\%$ as obtained from the normal-state data.

where H_{c2} is the upper critical field, $\beta \simeq 1.1$, and κ is the Ginzburg-Landau parameter. Using $\kappa \simeq 65$ (Ref. 32) and $H_{c2} \simeq 70$ kOe at $T = 0.3$ K, one obtains $4\pi\chi_d(1-n) \simeq -0.12\%$. This is a negative contribution to $K_\mu^{(\text{expt})}$ below T_c , which therefore cannot explain the observed positive change (Fig. 8). The data therefore indicate that $\chi_f(T)$ in undoped UBe_{13} decreases substantially below T_c at 5 kOe applied field independently of the diamagnetic correction (the magnitude of which would be decreased by flux trapping below T_c).

The behavior of the paramagnetic contribution χ_p to the susceptibility below T_c is also unknown; indeed, it is the spin-dependent contribution to χ_p which we wish to measure. Using as an upper bound the normal-state value $\chi_p \simeq 15 \times 10^{-3}$ emu mol $^{-1}$ at $T = 1.5$ K one obtains $4\pi(\frac{1}{3}-n)\chi_p \simeq 0.04\%$. This is smaller than the diamagnetic contribution and of opposite sign. Its change in the superconducting state, if any, would be in the same direction as the diamagnetic contribution. The observed change of $K_\mu^{(\text{expt})}$ is therefore a lower bound on the change of K_μ .

One of the most striking features of our results is the change of Knight-shift behavior with thorium doping.^{19,20,22} In the alloy $\text{U}_{1-x}\text{Th}_x\text{Be}_{13}$, $x = 0.033$, $|K_\mu|$ is constant or even increases slightly in the superconducting state (Fig. 8). A conventional explanation of this constancy would invoke a decrease with Th doping of the mean free path for spin-orbit scattering which, as mentioned previously, increases the spin susceptibility $\chi_s(T=0)$ to a nonzero value in conventional superconductors.^{31,33,34} Alternatively, the difference in shift behavior could be taken as evidence that the superconducting states for the two alloys are qualitatively different, i.e., that the pair symmetry is affected by Th doping. [An estimate of the diamagnetic correction to $K_\mu^{(\text{expt})}$ for $x = 0.033$ yields $4\pi\chi_d(1-n) \simeq -0.10\%$, which is similar to the value for $x = 0$ obtained above.]

To test this latter possibility we have measured K_μ in $\text{U}_{1-x}\text{Th}_x\text{Be}_{13}$ for the intermediate concentration $x = 0.01$.²² In this case K_μ was found to vary below T_c at a rate intermediate between the variations for $x = 0$ and 0.033 , as shown in Fig. 9. While not conclusive, these results suggest essentially conventional spin-orbit scattering by Th impurities. This suggests that in UBe_{13} the superconducting pairs are in spin-singlet states.

We now present a simple qualitative analysis of conventional spin-orbit scattering. From Fig. 9 it can be seen that the reduction of K_μ in the superconducting state of $\text{U}_{1-x}\text{Th}_x\text{Be}_{13}$ is suppressed for x of the order of 0.01. In conventional theory this suppression occurs for a mean free path $l_{s.o.}$ between spin-reversing scattering events of the order of the superconducting coherence length ξ_0 .³³ An estimate $\xi_0 \sim 100\text{--}150$ Å has been obtained from measurements of H_{c2} in UBe_{13} ,³⁷ so that $l_{s.o.}(x = 0.01) \sim 100$ Å. We can further estimate the mean free path l_{tr} for transport scattering events very roughly by assuming that the scattering is in the unitarity limit, which has some theoretical justification.³⁸ Then l_{tr} is of the order of the average distance between Th impurities, which for $x = 0.01$ yields $l_{tr} \sim 20$ Å or

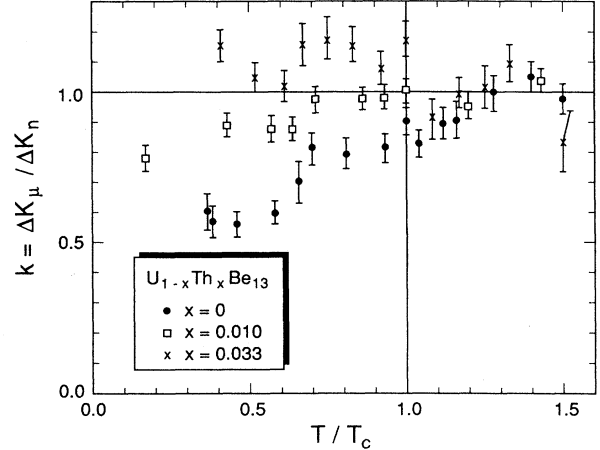


FIG. 9. Dependence of the reduced μ^+ Knight-shift change $k = \Delta K_\mu / \Delta K_n$ on reduced temperature T/T_c in superconducting $\text{U}_{1-x}\text{Th}_x\text{Be}_{13}$, $x = 0$ (●), 0.01 (□), and 0.033 (×). Here $\Delta K_\mu \equiv K_\mu^{(\text{expt})}(T) - K_\mu^{(\text{expt})}(\chi_f = 0)$, where $K_\mu^{(\text{expt})}(\chi_f = 0)$ is defined in the caption to Fig. 8, and ΔK_n is the average of ΔK_μ for $T/T_c \geq 1.2$.

$l_{s.o.}/l_{tr} \sim 5\text{--}10$.

The data are therefore consistent with one spin-reversing scattering event approximately every five to ten transport scattering events. This ratio is of the same order of magnitude as that obtained in conventional superconductors, most notably tin- and lead-based systems.³⁴ Thus the hypothesis of spin-orbit scattering is self-consistent in this sense. We will return to the question of the pairing symmetry in Sec. V below.

IV. EXPERIMENTAL RESULTS: (U,Th)Pt₃

Following the discovery of HF superconductivity in CeCu_2Si_2 and UBe_{13} , UPt_3 was also found to be superconducting³⁹ but with different and contrasting properties. The temperature dependence of the normal-state specific heat of UPt_3 at low temperatures was found to be indicative of strong spin fluctuations, which suggested that the superconducting mechanism might involve these fluctuations, i.e., be purely electronic in origin. In support of this picture, inelastic neutron scattering studies⁴⁰ found strong AF spin correlations in the normal state of UPt_3 . As mentioned in the introduction, doping UPt_3 with a few percent of thorium or palladium produces a sharp transition to an AF state.^{4,5} This suggests that UPt_3 possesses instabilities towards both magnetic and superconducting ground states, and is therefore an interesting system to study using μSR . Recently ^{195}Pt NMR in UPt_3 has been reported,⁴¹ we comment on these results below.

A. Relaxation-rate studies

Figure 10 shows the temperature dependence of the zero-, transverse-, and longitudinal-field linewidths in undoped UPt_3 between 0.17 and 300 K. The zero-field data were fit to the standard Kubo-Toyabe function [Eq. (4)]

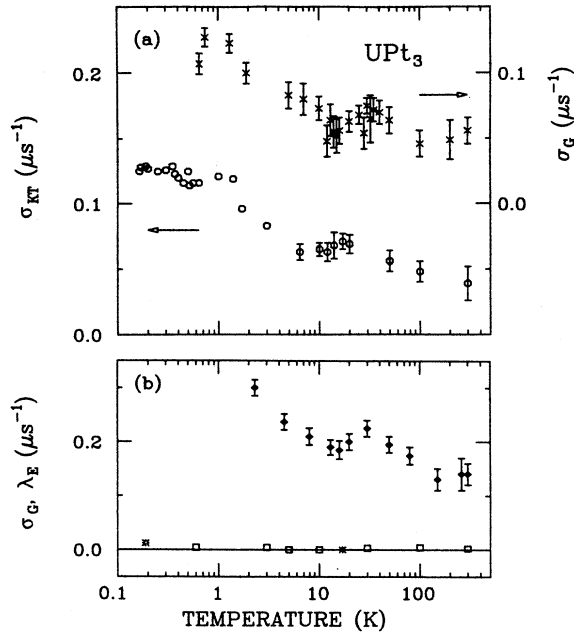


FIG. 10. Temperature dependence μ^+ linewidth is undoped UPt₃ between 0.17 and 300 K. (a) Zero-field Kubo-Toyabe linewidth σ_{KT} (○) and transverse-field (100 Oe) Gaussian linewidth σ_G (×). (b) Transverse-field (5 kOe) Gaussian linewidth σ_G (◆) and longitudinal-field Lorentzian linewidth (exponential relaxation rate) λ_E in 500 Oe (*) and 5 kOe (□). From Ref. 16.

to obtain σ_{KT} . Gaussian and exponential relaxation functions, $G_G(t) = \exp(-\frac{1}{2}\sigma_G^2 t^2)$ and $G_E(t) = \exp(-\lambda_E t)$, respectively, gave best fits to the transverse- and longitudinal-field data respectively. (The latter fit corresponds to a Lorentzian line shape, with linewidth λ_E .) This association of functional form with relaxation geometry is expected when transverse relaxation is due to a distribution of quasistatic local fields with a Gaussian distribution function, whereas longitudinal relaxation is caused by thermally excited fluctuations of the local field, i.e., by lifetime broadening, which gives a Lorentzian line shape. We first note that λ_E , taken in 0.5 and 5 kOe applied field (Fig. 10), was found to be zero within errors at all temperatures. This indicates the absence of spin-lattice or other dynamical relaxation mechanisms. Therefore the linewidths σ_G and σ_{KT} originate solely from inhomogeneous distributions of quasistatic local fields.

Values of the calculated Van Vleck linewidths σ_{VV} due to ¹⁹⁵Pt nuclear moments⁴² range between 0.031 and 0.042 μs^{-1} , depending on the assumed μ^+ interstitial site. (The contribution of U nuclear moments to σ_{VV} is negligible.) Thus the Kubo-Toyabe linewidth $\sigma_{KT} = \sqrt{5/2}\sigma_{VV}$ in zero field for a stationary muon should range between 0.049 and 0.066 μs^{-1} , which is consistent with our measurements above ~ 6 K. The decrease in linewidth above ~ 30 K is probably due to slow muon hopping.

We note, however, that at all temperatures the rates

σ_G in 100 Oe transverse field are nearly the same magnitude as the zero-field rates σ_{KT} . This would not be expected from nuclear broadening alone, since ¹⁹⁵Pt nuclei ($I = \frac{1}{2}$) possess no nuclear quadrupole moment (cf. the discussion of quadrupole effects in Sec. II A). In addition, σ_G increases by a factor of 2–3 as H_0 is increased from 100 Oe to 5 kOe.

Below 5–6 K σ_{KT} increases monotonically as the temperature is reduced, and reaches a plateau below ~ 0.5 –1 K, similar to the order parameter obtained from neutron scattering.⁴³ Qualitatively similar behavior is seen in the transverse-field data, except that the increase of σ_G begins at a slightly higher temperature (~ 10 K). There is some indication of a slight additional increase of σ_{KT} below T_c , but an unambiguous effect has not been resolved. The low-temperature values of σ_{KT} and σ_G are approximately a factor of 2 greater than can be accounted for by nuclear broadening.

These results imply an additional source of μ^+ local field, for which we now consider the following mechanisms: (1) a magnetic second phase, (2) a strong Ruderman-Kittel-Kasuya-Yosida (RKKY)-type coupling between μ^+ and ¹⁹⁵Pt moments, motionally narrowed at higher temperatures by rapid ¹⁹⁵Pt Korringa relaxation, and (3) heavy-fermion magnetism. We discuss these in turn.

a. Magnetic second phase. Magnetization measurements were performed on a portion of the sample used for μSR to determine the possible existence of a magnetic second phase. No remanent magnetization greater than $\sim 2 \times 10^{-3}$ emu g⁻¹ was observed. If UPt ($T_c = 27$ K) is assumed to be the ferromagnetic second phase,¹⁴ it must be present at less than 0.065% mole fraction.

The Walstedt-Walker (WW) mechanism⁴⁵ for inhomogeneous line broadening in a random alloy of static paramagnetic impurities is also applicable to broadening by dipolar fields from inclusions of a magnetic second phase, as long as the inclusions are small and randomly dispersed. The Lorentzian linewidth (exponential relaxation rate) λ_E in the WW calculation is then given by $\lambda_E = 5.065\gamma_\mu m_{\text{eff}}$, where m_{eff} is the magnetization of the second phase averaged over the entire sample. If a maximum UPt concentration of 0.065% is assumed, based on the magnetization measurements, then the WW calculation yields $\lambda_E \lesssim 0.016 \mu\text{s}^{-1}$. A fit of the relaxation data below 2 K to an exponential relaxation function yields $\lambda_E \simeq 0.057 \mu\text{s}^{-1}$. We conclude, therefore, that the contribution to the observed μ^+ linewidth from magnetic inclusions is small at best. Furthermore, there are no known magnetic phases in the U-Pt alloy system with ordering temperatures of 5–6 K.

b. Indirect μ^+ -nuclear interactions. We now consider the consequences of a strong electron-mediated (RKKY) indirect interaction between μ^+ and ¹⁹⁵Pt nuclear moments. Such an indirect interaction has been shown to exist, for example, between μ^+ and Mn moments in AgMn alloys.⁴⁶ The order of magnitude of the μ^+ linewidth σ_{ind} due to this indirect mechanism is⁴⁷

$$\sigma_{\text{ind}} \simeq A_\mu A_{\text{Pt}} \rho(\epsilon_F), \quad (8)$$

where A_μ and A_{Pt} are the hyperfine coupling constants (in units of frequency) between band electrons and the μ^+ and ^{195}Pt spins, respectively, and $\rho(\epsilon_F)$ is the density of band states at the Fermi energy (in units of time).

A value $\sigma_{\text{ind}} \approx 10^5 \text{ s}^{-1}$ is required to explain the observed μ^+ linewidth in UPt_3 at low temperatures. Recent ^{195}Pt NMR measurements⁴¹ in UPt_3 obtain a transferred hyperfine field $H_{\text{hf}}(\text{Pt})$ of $-100 \text{ kOe}/\mu_B$, which yields $A_{\text{Pt}} = \gamma_{\text{Pt}} H_{\text{hf}}(\text{Pt}) = 5.8 \times 10^8 \text{ s}^{-1}$. Here γ_{Pt} is the ^{195}Pt nuclear gyromagnetic ratio. From our μ^+ Knight-shift measurements (cf. Sec. IV B below) we obtain $A_\mu \approx 8.5 \times 10^6 \text{ s}^{-1}$. The density of states in UPt_3 can be estimated from the measured specific-heat linear coefficient $\gamma = 260 \text{ mJ mol}^{-1} \text{ K}^{-2}$ to be $\rho(\epsilon_F) \sim 4 \times 10^{-14} \text{ s}$. The estimated value of σ_{ind} is therefore of order 10^2 s^{-1} , which is a factor of 1000 smaller than the required value. Therefore an indirect interaction cannot be the explanation for the observed enhancement.

c. Heavy-fermion magnetism. Finally, we examine the consequences of assumed quasistatic magnetic order in the heavy-electron system. As noted in Sec. III A, μ^+ hyperfine fields via either dipolar or transferred (indirect contact) mechanisms are typically in the range 1–10 kOe/μ_B . Thus the observed increase of linewidth below 6 K of $\sim 1 \text{ Oe}$ in field units implies a very small moment per U atom, similar to (and subject to the same caveat regarding site symmetry as) that discussed above in the case of $(\text{U,Th})\text{Be}_{13}$. If the linewidth were due to itinerant magnetism only a small fraction of the Fermi surface might be involved, and such a magnetic phase transition might not be readily visible in, for example, specific-heat, magnetization, or resistivity measurements. To our knowledge no anomalies have been reported in these quantities near 6 K. But the temperature derivative $d\rho/dT$ of the resistivity shows a broad peak near 5–6 K in single-crystal UPt_3 ⁴⁸ which shifts upwards a few degrees under a pressure of 4.2 kbar. Similarly, the temperature dependence of the magnetoresistance shows a broad peak in the same temperature range,⁴⁸ which is itself a maximum as a function of field near 200 kOe. These measurements suggest a weak magnetic anomaly in the same temperature region where our μSR results show an increase in linewidth.

Preliminary reports^{21,22} of our results stimulated searches for low-temperature magnetic order in UPt_3 using neutron scattering. Recently Aeppli *et al.*⁴³ have reported the observation of very weak AF order in UPt_3 over a temperature range which roughly agrees with that for which the μSR linewidth increases. The magnetic structure obtained from this study is the same as that seen in $(\text{U,Th})\text{Pt}_3$, although the ordered moment of $\sim 10^{-2} \mu_B$ is considerably lower than in the latter alloy. However, attempts by other investigators to reproduce these results have not been consistent: apparently some samples show the effect and some do not.⁴⁹

We now discuss zero-field relaxation-rate measurements in $\text{U}_{1-x}\text{Th}_x\text{Pt}_3$, $x=0.01$ and 0.05. Zero-field asymmetries, relaxation rates, and frequencies for $x=0.05$ are shown in Fig. 11 for temperatures between 3.4 and 10 K. Below 6.5–7 K two frequency components

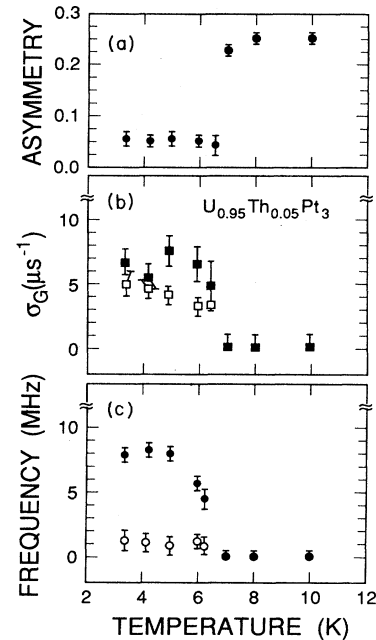


FIG. 11. Temperature dependence of (a) asymmetry, (b) linewidths σ_G , and (c) zero-field frequencies in $\text{U}_{0.95}\text{Th}_{0.05}\text{Pt}_3$.

spontaneously appear in the zero-field relaxation spectra. This is clear evidence for a strong and relatively homogeneous internal field at some μ^+ sites for $T \lesssim 6.5 \text{ K}$, which is consistent with earlier transport and thermodynamic evidence⁴ for a magnetic phase transition at this temperature. The zero-field precession is accompanied by a decrease in the overall asymmetry from ~ 0.25 to ~ 0.05 , together with an increase in the Gaussian linewidth of each component, as the temperature is decreased.

We interpret these results as follows. The appearance of more than one precession frequency is evidence for more than one μ^+ lattice site. The fact that the full asymmetry observed above 7 K is not maintained in the precessing components below 6.5 K indicates either that a majority of the stopped muons are depolarized in a time short compared to the spectrometer “dead” time of $\sim 25 \text{ ns}$, or that very-high-frequency components ($\geq 100 \text{ MHz}$) are present which are not resolved in our experiments. In either case more than two μ^+ sites are implied. The positions of these sites can only be determined by experiments on single crystals and from data of greater statistical accuracy than is readily available in our apparatus. Nevertheless the present data show clear evidence for the onset of static magnetic order.

The higher of the two observed frequencies ($\sim 8 \text{ MHz}$ at $T=4 \text{ K}$) increases monotonically with decreasing temperature, which mirrors the growth of the order parameter or local magnetic field. A frequency of 8 MHz corresponds to a local field of about 600 Oe which, assuming dipolar coupling ($\sim 1 \text{ kOe}/\mu_B$), implies an upper limit of about $0.6 \mu_B/\text{U}$ atom to the AF sublattice magnetization. In the absence of a μ^+ site determination this can only be

considered an estimate, although it agrees well with the neutron diffraction result.⁶ We also note that for the 8-MHz line the linewidth σ_G is of the same order as the precession frequency, which indicates that there is a broad distribution of μ^+ local fields. Since the neutron-diffraction data reveal a commensurate FM spin structure, this field distribution may be due to defect-induced perturbations of the μ^+ sites.

We also obtained μ SR data for $U_{1-x}Th_xPt_3$, $x=0.01$. As can be seen from Fig. 12, no evidence for a magnetic phase transition is found from the transverse-field linewidths. Indeed, the data for $x=0.01$ are consistent with those for undoped UPt_3 (Fig. 10) over the temperature range 4–22 K, although there are not enough data to determine the presence of weak magnetic order below ~ 5 K in this sample.

B. Knight shift in UPt_3

Muon Knight-shift and susceptibility measurements were carried out in UPt_3 over the temperature range 2–150 K. The results are shown in Fig. 13, where it can be seen that $K_\mu^{(expt)}$ is proportional to the bulk susceptibility χ over the entire temperature range. Comparison with Fig. 7 reveals that $K_\mu^{(expt)}$ is 1 to 2 orders of magnitude smaller in UPt_3 than in $(U,Th)Be_{13}$, although the powder-averaged susceptibility is only about a factor of 2 smaller. We also find that $K_\mu^{(expt)}$ is dominated by the Lorentz and demagnetization terms calculated from Eqs. (6) and (7), which give a contribution of $0.068 \text{ mol emu}^{-1}$ to the observed slope $0.086 \pm 0.014 \text{ mol emu}^{-1}$ (Fig. 13). These data yield a value $100 \pm 80 \text{ Oe}/\mu_B$ for the hyperfine field, which is an order of magnitude smaller than in UBe_{13} . Such a reduction could possibly be due to the existence of unresolved signals from multiple μ^+ stopping sites with transferred hyperfine couplings of opposite sign.

V. SUMMARY AND CONCLUSIONS

This paper has presented a study of microscopic aspects of magnetism and superconductivity in the heavy-

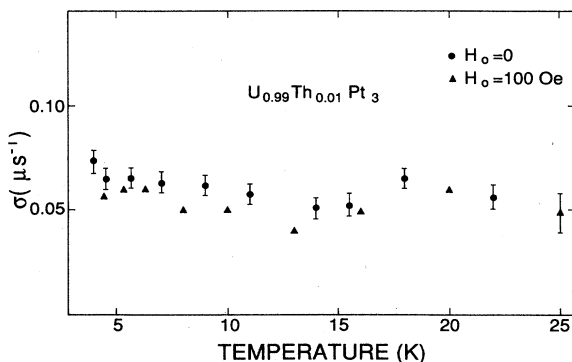


FIG. 12. Temperature dependence of the zero-field Kubo-Toyabe linewidth σ_{KT} (●) and the transverse-field (100 Oe) Gaussian linewidth σ_G (◆) in $U_{0.99}Th_{0.01}Pt_3$.

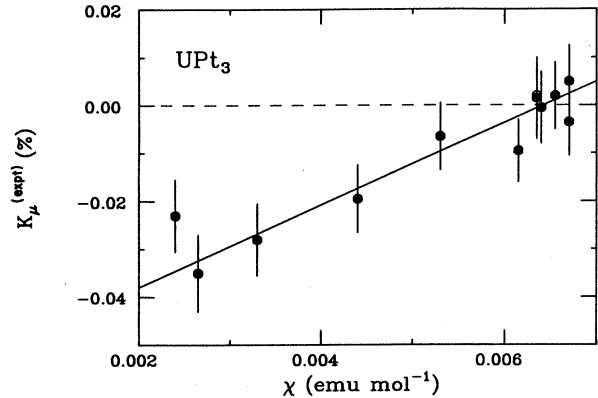


FIG. 13. Dependence of the experimental μ^+ Knight shift $K_\mu^{(expt)}$, not corrected for Lorentz and demagnetizing fields, on bulk susceptibility χ in the normal state of UPt_3 . Temperature is an implicit variable. Solid line: best linear fit, slope is $0.086 \pm 0.014 \text{ mol emu}^{-1}$.

fermion alloy systems $(U,Th)Be_{13}$ and $(U,Th)Pt_3$ using the μ SR technique.

In undoped UBe_{13} the μ^+ Gaussian transverse relaxation rate σ_G is roughly independent of temperature below ~ 150 K, but exhibits motional narrowing at higher temperatures due to thermally activated μ^+ diffusion. The observed value of σ_G is consistent with relaxation by coupling to 9Be nuclear dipole moments for several candidate μ^+ interstitial sites. The zero-field relaxation rate σ_{KT} in UBe_{13} is also independent of temperature below ~ 3 K and nearly equal to σ_G . This near equality is expected, at least qualitatively, if nonsecular terms in the dipolar interaction between μ^+ and 9Be nuclear moments are averaged by 9Be precession in preexisting crystalline EFG's.

In $U_{1-x}Th_xBe_{13}$, $x=0.033$, a significant increase of σ_{KT} is observed below the temperature $T_{c2} \approx 0.4$ K at which a second phase transition occurs in the superconducting state. This jump is firm evidence that weak static magnetism is associated with the phase transition at T_{c2} . The increase in local field at μ^+ sites, ~ 1.5 Oe, corresponds to an effective moment of $10^{-3} - 10^{-2} \mu_B/U$ atom. It is still an open question whether or not this is the same general kind of weak magnetic order as has been observed in the normal state of UPt_3 and other heavy-fermion systems,^{17,18} or if, alternatively, it is associated with a nonunitary superconducting state. The former possibility might be related to an inherent instability against formation of a spin-density wave, as discussed by Machida and Kato.⁵⁰ Consequences of nonunitary states have been treated by Sigrist and Rice,²⁹ although they consider only a nonzero Cooper-pair spin polarization density for odd-parity (triplet) pairing. The observed large reduction of the μ^+ Knight shift in undoped UBe_{13} (cf. Sec. III B and below) appears to be evidence against triplet pairing, at least for $x=0$, and a change of pair symmetry from singlet to triplet with Th doping does not appear to be likely. Nonunitary superconducting states also occur for singlet (*d*-wave-like) pairing, however. In

this case the spin polarization vanishes, but orbital currents might cause the observed increase in μ^+ linewidth. This possibility requires further theoretical work.

The μ^+ Knight shift K_μ in the normal states $U_{1-x}\text{Th}_x\text{Be}_{13}$, $x=0$ and 0.033, varies linearly with the bulk susceptibility, and yields an f -spin transferred μ^+ hyperfine field of -1.99 ± 0.12 kOe/ μ_B . In the superconducting states of these materials a large reduction of the magnitude of K_μ is observed for $x=0$. For $x=0.033$ no reduction of K_μ is observed, and an intermediate reduction is found for $x=0.01$. This behavior suggests (1) spin-singlet pairing in undoped UBe_{13} and (2) a conventional increase of the superconducting spin susceptibility in $(\text{U,Th})\text{Be}_{13}$ by spin-orbit scattering from Th impurities (as well as some residual spin-orbit scattering in nominally pure UBe_{13}). Assuming conventional theory the mean free path $l_{\text{s.o.}}$ for spin-orbit scattering can be estimated, and is of the same order of magnitude relative to the transport mean free path l_{tr} ($l_{\text{s.o.}}/l_{\text{tr}} \simeq 5-10$) as in conventional superconductors.

In undoped UPt_3 small increases of σ_G and σ_{KT} below ~ 6 K are again evidence for the onset of weak static magnetism similar to that found in $(\text{U,Th})\text{Be}_{13}$. Recent spin-polarized neutron scattering studies⁴³ have

confirmed this: a commensurate AF structure with a sublattice magnetization of $\sim 10^{-2} \mu_B/\text{U}$ atom was found, in rough agreement with the μSR results. For $x=0.05$ large zero-field μ^+ precession frequencies below 6.5 K indicate an AF structure with a considerably larger moment: $\sim 0.6 \mu_B/\text{U}$ atom. This result confirms earlier determinations of magnetic order in this system from bulk measurements⁴ and neutron scattering.⁶ The μ^+ Knight shift in the normal state of UPt_3 was found to be much smaller than in UBe_{13} ; nearly all the observed shift could be accounted for by demagnetization fields rather than microscopic contributions.

ACKNOWLEDGMENTS

We are grateful to S. A. Dodds for help with the data acquisition, and to J. A. Flint for help in the data analysis. This work was supported in part by National Science Foundation Grant No. DMR-8413730, the University of California, Riverside, Academic Senate Committee on Research, the Association of Western Universities, the San Jose State Foundation, and the Robert A. Welch Foundation. The work was also performed in part under the auspices of the Department of Energy.

¹General reviews: G. R. Stewart, *Rev. Mod. Phys.* **56**, 755 (1984); Z. Fisk, H. R. Ott, T. M. Rice, and J. L. Smith, *Nature (London)* **320**, 124 (1986); Z. Fisk, D. W. Hess, C. J. Pethick, D. Pines, J. L. Smith, J. D. Thompson, and J. O. Willis, *Science* **239**, 33 (1988).

²Review of theory: P. A. Lee, T. M. Rice, J. W. Serene, L. J. Sham, and J. W. Wilkins, *Comments Cond. Matter. Phys.* **12**, 99 (1986).

³J. P. Brison, A. Ravex, J. Flouquet, Z. Fisk, and J. L. Smith in *Proceedings of the 6th International Conference on Crystal-Field Effects and Heavy-Fermion Physics* [*J. Magn. Magn. Mater.*, **76-77**, 525 (1988)]; see also Ref. 11.

⁴A. P. Ramirez, B. Batlogg, E. Bucher, and A. S. Cooper, *Phys. Rev. Lett.* **57**, 1072 (1986).

⁵A. de Visser, J. C. P. Klaasse, M. van Sprang, J. J. M. Franse, A. Menovsky, and T. T. M. Palstra, *J. Magn. Magn. Mater.* **54-57**, 375 (1986); G. R. Stewart, A. L. Giorgi, J. O. Willis, and J. O'Rourke, *Phys. Rev. B* **34**, 4629 (1986).

⁶A. I. Goldman, G. Shirane, G. Aeppli, B. Batlogg, and E. Bucher, *Phys. Rev. B* **34**, 6564 (1986).

⁷J. L. Smith, Z. Fisk, J. O. Willis, B. Batlogg, and H. R. Ott, *J. Appl. Phys.* **55**, 1996 (1984).

⁸H. R. Ott, H. Rudigier, Z. Fisk, and J. L. Smith, *Phys. Rev. B* **31**, 1651 (1985).

⁹B. Batlogg, D. Bishop, B. Golding, C. M. Varma, Z. Fisk, J. L. Smith, and H. R. Ott, *Phys. Rev. Lett.* **55**, 1319 (1985).

¹⁰G. Aeppli (private communication).

¹¹D. E. MacLaughlin, C. Tien, W. G. Clark, M. D. Lan, Z. Fisk, J. L. Smith, and H. R. Ott, *Phys. Rev. Lett.* **53**, 1833 (1984).

¹²For a review of the μSR technique see A. Schenck, *Muon Spin Rotation Spectroscopy* (Adam Hilger, Bristol, 1985). The use of positive muons in metal physics is reviewed by E.

Karlsson, *Phys. Rep.* **82**, 271 (1982). (See also references contained in these articles.)

¹³S. Barth, H. R. Ott, F. N. Gygax, A. Schenck, T. M. Rice, and Z. Fisk, *Hyperfine Interact.* **31**, 397 (1986).

¹⁴S. Barth, H. R. Ott, F. Hulliger, F. N. Gygax, A. Schenck, and T. M. Rice, *Hyperfine Interact.* **31**, 403 (1986).

¹⁵Y. J. Uemura, W. J. Kossler, B. Hitti, J. R. Kempton, H. E. Schone, X. H. Yu, C. E. Stronach, W. F. Lankford, D. R. Noakes, R. Keitel, M. Senba, J. H. Brewer, E. J. Ansaldo, Y. Oonuki, T. Komatsubara, G. Aeppli, E. Bucher, and J. E. Crow, *Hyperfine Interact.* **31**, 413 (1986).

¹⁶D. E. MacLaughlin, D. W. Cooke, R. H. Heffner, R. L. Hutson, M. W. McElfresh, M. E. Schillaci, H. D. Rempp, J. L. Smith, J. O. Willis, E. Zirngiebl, C. Boekema, R. L. Lichti, and J. Oostens, *Phys. Rev. B* **37**, 3153 (1988).

¹⁷S. Barth, H. R. Ott, F. N. Gygax, B. Hitti, E. Lippelt, A. Schenck, C. Baines, B. van den Brandt, T. Konter, and S. Mango, *Phys. Rev. Lett.* **59**, 2991 (1987).

¹⁸Y. J. Uemura, W. J. Kossler, X. H. Yu, H. E. Schone, J. R. Kempton, C. E. Stronach, S. Barth, F. N. Gygax, B. Hitti, A. Schenck, C. Baines, W. F. Lankford, Y. Onuki, and T. Komatsubara, *Physica B+C* **153-155C**, 455 (1988).

¹⁹R. H. Heffner, D. W. Cooke, Z. Fisk, R. L. Hutson, M. E. Schillaci, J. L. Smith, J. O. Willis, D. E. MacLaughlin, C. Boekema, R. L. Lichti, A. B. Denison, and J. Oostens, *Phys. Rev. Lett.* **57**, 1255 (1986).

²⁰R. H. Heffner, D. W. Cooke, Z. Fisk, R. L. Hutson, M. E. Schillaci, J. L. Smith, J. O. Willis, D. E. MacLaughlin, C. Boekema, R. L. Lichti, A. B. Denison, and J. Oostens, *Hyperfine Interact.* **31**, 419 (1986).

²¹D. W. Cooke, R. H. Heffner, R. L. Hutson, M. E. Schillaci, J. L. Smith, J. O. Willis, D. E. MacLaughlin, C. Boekema, R. L.

- Lichti, A. B. Denison, and J. Oostens, *Hyperfine Interact.* **31**, 425 (1986).
- ²²R. H. Heffner, D. W. Cooke, and D. E. MacLaughlin, in *Theoretical and Experimental Aspects of Valence Fluctuations and Heavy Fermions*, edited by L. C. Gupta and S. K. Malik (Plenum, New York, 1987), p. 319.
- ²³A. Schenck, *Helv. Phys. Acta* **54**, 471 (1981).
- ²⁴D. W. Cooke, J. K. Hoffer, M. Maez, W. A. Steyert, and R. H. Heffner, *Rev. Sci. Instrum.* **57**, 336 (1986).
- ²⁵R. S. Hayano, Y. J. Uemura, J. Imazato, H. Nishida, T. Yamazaki, and R. Kubo, *Phys. Rev. B* **20**, 850 (1979).
- ²⁶W. G. Clark, M. D. Lan, G. van Kalker, W. H. Wong, C. Tien, D. E. MacLaughlin, J. L. Smith, Z. Fisk, and H. R. Ott, *J. Magn. Magn. Mater.* **63-64**, 396 (1987).
- ²⁷H. R. Ott, H. Rudigier, E. Feldner, Z. Fisk, and J. L. Smith, *Phys. Rev. B* **33**, 126 (1986).
- ²⁸G. E. Volovik and L. P. Gor'kov, *Zh. Eksp. Teor. Fiz.* **88**, 1412 (1985) [*Sov. Phys.—JETP* **61**, 842 (1985)].
- ²⁹M. Sigrist and T. M. Rice, in Ref. 3, p. 487.
- ³⁰See, e.g., G. C. Carter, L. H. Bennett, and D. J. Kahan, *Prog. Mater. Sci.* **20**, 1 (1977).
- ³¹For reviews see R. Meservey and B. B. Schwartz, in *Superconductivity*, edited by R. D. Parks (Dekker, New York, 1969); D. E. MacLaughlin in *Solid State Physics*, edited by H. Ehrenreich, F. Seitz, and D. Turnbull (Academic, New York, 1976), Vol. 31, and references therein.
- ³²K. Yosida, *Phys. Rev.* **110**, 769 (1958).
- ³³R. A. Ferrell, *Phys. Rev. Lett.* **3**, 262 (1959); P. W. Anderson, *ibid.* **3**, 325 (1959).
- ³⁴F. Wright, W. A. Hines, and W. D. Knight, *Phys. Rev. Lett.* **18**, 115 (1967); W. A. Hines and W. D. Knight, *Phys. Rev. B* **4**, 893 (1971). See also Ref. 25.
- ³⁵A. J. Leggett, *Rev. Mod. Phys.* **47**, 331 (1975).
- ³⁶J. A. Cape and J. M. Zimmerman, *Phys. Rev.* **153**, 416 (1967).
- ³⁷M. B. Maple, J. W. Chen, S. E. Lambert, Z. Fisk, J. L. Smith, H. R. Ott, J. S. Brooks, and M. J. Naughton, *Phys. Rev. Lett.* **54**, 477 (1985); U. Rauchschwalbe, *Physica (Amsterdam)* **147B**, 1 (1987).
- ³⁸C. J. Pethick and D. Pines, *Phys. Rev. Lett.* **57**, 118 (1986).
- ³⁹G. R. Stewart, Z. Fisk, J. O. Willis, and J. L. Smith, *Phys. Rev. Lett.* **52**, 679 (1984).
- ⁴⁰G. Aeppli, A. Goldman, G. Shirane, E. Bucher, and M. Ch. Lux-Steiner, *Phys. Rev. Lett.* **58**, 808 (1987).
- ⁴¹Y. Kohori, T. Kohara, H. Shibai, Y. Oda, T. Kaneko, Y. Kitaoka, and K. Asayama, *J. Phys. Soc. Jpn.* **56**, 2263 (1987).
- ⁴²See, e.g., A. Abragam, *The Principles of Nuclear Magnetism* (Clarendon, Oxford, 1961), Chap. IV.
- ⁴³G. Aeppli, E. Bucher, C. Broholm, J. K. Kjems, J. Baumann, and J. Hufnagl, *Phys. Rev. Lett.* **60**, 615 (1988).
- ⁴⁴P. H. Frings, J. J. M. Franse, F. R. de Boer, and A. Menovsky, *J. Magn. Magn. Mater.* **31-34**, 240 (1983).
- ⁴⁵R. E. Walstedt and L. R. Walker, *Phys. Rev. B* **9**, 4857 (1974).
- ⁴⁶R. H. Heffner, D. W. Cooke, R. L. Hutson, M. E. Schillaci, S. A. Dodds, G. A. Gist, and D. E. MacLaughlin, *J. Magn. Magn. Mater.* **54-57**, 1103 (1986).
- ⁴⁷See, for example, A. Abragam, *The Principles of Nuclear Magnetism*, Ref. 42, pp. 206–210.
- ⁴⁸A. de Visser, J. J. M. Franse, and A. Menovsky, *J. Magn. Magn. Mater.* **43**, 43 (1984); A. de Visser, R. Gersdorf, J. J. M. Franse, and A. Menovsky, *ibid.* **54-57**, 383 (1986).
- ⁴⁹J. J. M. Franse (private communication).
- ⁵⁰K. Machida and J. Kato, *Phys. Rev. Lett.* **58**, 1986 (1988); M. Kato and K. Machida, *Phys. Rev. B* **37**, 1510 (1988).